Size-Control and Optical Properties of Organic Nanocrystals

ARTICLE *in* JOURNAL OF NANOSCIENCE AND NANOTECHNOLOGY · MARCH 2009

Impact Factor: 1.56 · DOI: 10.1166/jnn.2009.C140 · Source: PubMed

4 AUTHORS, INCLUDING:

Mei-Ling Zheng
Technical Institute of Physics and Chemistry
55 PUBLICATIONS **297** CITATIONS

SEE PROFILE

THE JOURNAL OF PHYSICAL CHEMISTRY C

ARTICLE

pubs.acs.org/JPCC

Two-Photon Excited Fluorescence and Second-Harmonic Generation of the DAST Organic Nanocrystals

Mei-Ling Zheng,[†] Katsumasa Fujita,[*,‡] Wei-Qiang Chen,[†] Xuan-Ming Duan,[*,†] and Satoshi Kawata[‡]

[†]Laboratory of Organic NanoPhotonics and Key Laboratory of Functional Crystals and Laser Technology, Technical Institute of Physics and Chemistry, Chinese Academy of Sciences, Zhongguancunbeiyitiao No. 2, Beijing 100190, P. R. China

[‡]Department of Applied Physics, Osaka University, 2-1Yamadaoka, Suita, Osaka 565-0871, Japan

Supporting Information

ABSTRACT: The nonlinear optical properties of the size-controlled *trans*-4-[4-(dimethylamino)-*N*-methylstilbazolium] *p*-tosylate (DAST) organic nanocrystals (ONCs) have been investigated. The size and monoclinic crystal structure have been demonstrated by the scanning electron microscope, transmission electron microscope, and X-ray diffraction measurement. The DAST ONCs exhibited 6-fold enhanced fluorescence quantum yield and prolonged fluorescence lifetime compared to DAST molecular solution. The evaluations of two-photon excited fluorescence (TPEF) and second-harmonic generation (SHG) microscopes have been implemented for investigating the optical nonlinearities of DAST nanocrystals. The TPEF intensity of DAST ONCs was improved by a factor of 37.3 compared to DAST molecular solution. The extraordinary large two-photon absorption cross section up to 1.72×10^6 GM was observed. DAST ONC was demonstrated as a single crystal from the four-lobe polarization response in the SHG microscope. These results would provide DAST ONCs the opportunity for the potential application in photonics and bioimaging as nonlinear optical materials.

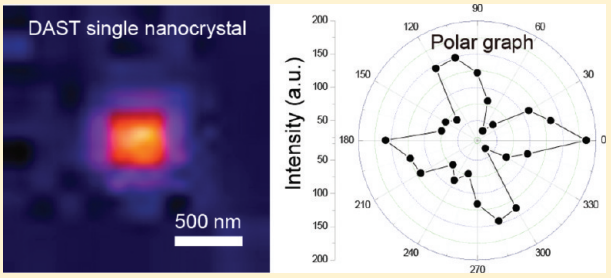

INTRODUCTION

Development of organic materials with excellent nonlinear optical (NLO) properties has been a highly active area of researches for a wide variety of promising applications, including optical limiting, up-converted lasing, 3D optical data storage and microfabrication, bioimaging, and photodynamic therapy.[1−3] Until now, the investigations on the optical nonlinearities including two-photon excited fluorescence (TPEF) property and polarization response in the second-harmonic generation (SHG) have been done in solutions, dye-doped films, and bulk crystals.[4,5] It is well-known that organic nanocrystals (ONCs) show not only size-dependent multicolor emission but also aggregation-enhanced fluorescence.[6−8] However, further investigation of the NLO properties of ONCs has been hindered. The major issues for fluorescent nanoprobes include the low two-photon absorption cross section (δ), the aggregation-induced fluorescence quenching,[9,10] and the low hyperpolarizability.[11] If the performances of individual nonlinear optical molecules can be cooperatively enhanced within the highly localized nanostructure, the nanocrystals would be of high utility as TPEF and SHG probes.

Compared to neutral analogous, π-conjugated dipolar organic salts possess larger electro-optical and NLO response as well as better photostability and thermal stability. The usage of NCs of organic salts as NLO probes could not only utilize their large NLO properties but also improve their photostability and thermal stabilitiy. *trans*-4-[4-(dimethylamino)-*N*-methylstilbazolium] *p*-tosylate, DAST, has been widely studied as organic nonlinear material due to its high electro-optical and NLO response.[12−16] However, ONCs of DAST with the size less than 100 nm attracted very little attention in their photoluminescence due to the preparation difficulty caused by their excellent crystalline capability.[17] In our previous work,[18,19] we found that silicon-based dendrimers[20−22] had excellent site-isolation effect for ionic molecules, which was promising for controlling the kinetic growing process. We succeeded to achieve nanoscale ONCs by using carbosiloxane dendrimer to control the growth process of DAST crystal,[20] which would provide the suitable material of high quality for investigating the optical nonlinearity of ONCs.

For better understanding the optical property of DAST crystals at nanometric scale and discovering their potential application in nonlinear optics and imaging, we have investigated the crystal structure and the optical nonlinearities of the DAST ONCs in this study. The monoclinic crystal structure was demonstrated by transmission electron microscope (TEM) and the X-ray diffraction (XRD) characterization. The enhanced TPEF and the four-lobe polarization response were achieved from the DAST ONCs. This result would open up broad

Received: March 11, 2011
Revised: April 8, 2011
Published: April 19, 2011

prospects for the application of DAST ONCs in the field of fluorescent sensing as nonlinear optical nanoprobes.

EXPERIMENTAL SECTION

Measurements. The scanning electron microscopy (SEM) images of DAST ONCs were acquired on Hitachi S-4300 FEGd scanning electron microscopy. The SEM samples of the DAST ONCs were prepared by dropping the suspension of the DAST ONCs onto a slide glass and allowed the solvent to evaporate at room temperature. Then the samples were covered with aurums by a vacuum coat. The morphology and sizes of DAST ONCs were determined by TEM (JEM-2010). The crystal structure of DAST ONCs was characterized by XRD (D8 Focus, Bruker, Germany).

Scheme 1. Schematic Diagram of the Second-Harmonic Generation (SHG) Microscope

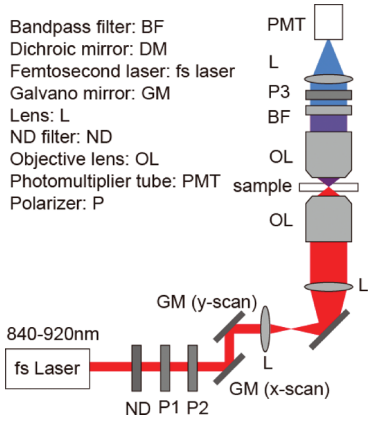

The UV−vis absorption and fluorescence emission spectra of DAST ONCs were recorded on a Shimadzu UV-2500 spectrophotometer and a Hitachi FL-4500 spectrophotometer, respectively. The fluorescence quantum yield was calculated using fluorescein in 0.1 N aqueous NaOH solution (Φ = 0.9) as a reference standard. Both of the DAST ONCs and DAST methanol solution were excited at 480 nm. Time-resolved fluorescence measurements were performed using a streak scope camera (Hamamatsu, C4334) with the excitation of femtosecond laser pulse at the wavelength of 400 nm. The time resolution of the system was about 10 ps limited by the streak camera. The emission spectra of the solid DAST ONCs were measured by a steady state fluorimeter (FS920, Edinburgh Instrument).

Two-photon excited induced fluorescence emission were recorded on a SD2000 spectrometer (Ocean Optics) using a femtosecond mode-locked Ti:sapphire laser (Tsunami, Spectra-Physics) as the excitation source. The oscillating wavelength, pulse width, and repetition rate were of 780 nm, 80 fs, and 82 MHz, respectively.

The polarization dependence of DAST ONCs were measured by a homemade SHG microscope (Scheme 1). Chameleon diode-pumped femtosecond laser (Coherent) with the wavelength of 870 nm, repetition rate of 90 MHz, and pulse width of 140 fs was used as the light source. The microscope consisting of galvanometer mounted mirrors (MiniSAX, GSI) was used for beam scanning, realizing the $x-y$ plane scan. Polarizers (P) P1 and P2 were used to tune the polarization direction of excitation laser source. P3 was used to change the polarization direction of detection. The objective lens were Olympus, PlanAPO, 60×, N. A. 1.0, water (bottom) and Olympus UMplanFI 100×, N.A. 0.95 (up). The SHG signal was detected by photomultiplier tube (PMT, H7710-13, Hamamatsu) in the forward direction. A bandpass filter FF01-434-17/25 (Semrock) was used to remove the excitation laser light.

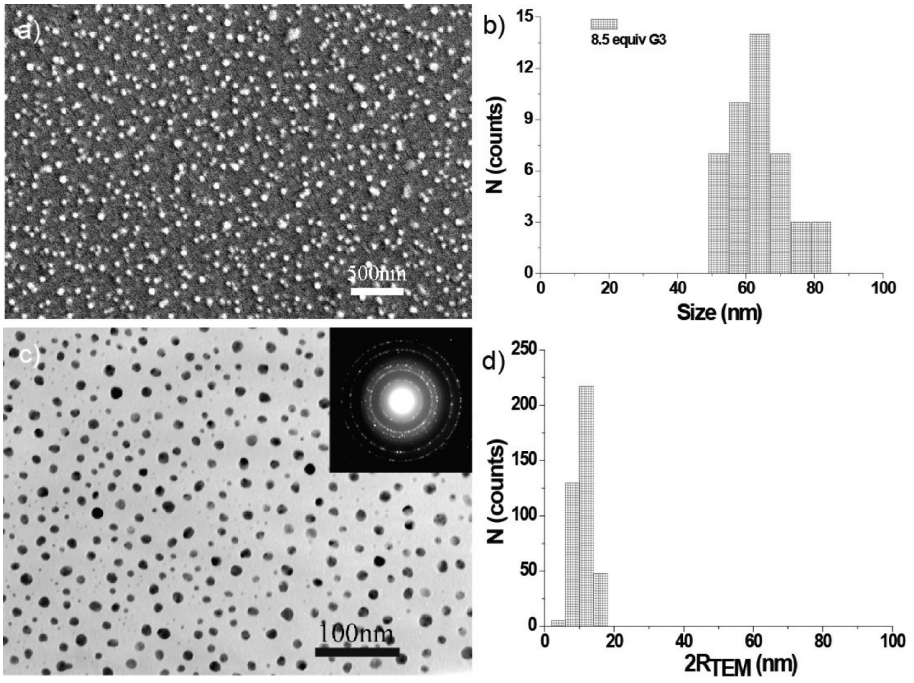

Figure 1. (a) SEM images of DAST ONCs prepared with CSiO-G3. CSiO-G3/DAST = 8.5:1 with the average sizes of 65 ± 15 nm ([DAST] = 2.0 × 10^{-5} M). The scale bar represented 500 nm. (c) TEM images of DAST ONCs ([DAST] = 2.0 × 10^{-5} M, CSiO-G3/DAST = 8.5:1); the scale bar represents 100 nm. Inset shows the electron diffraction pattern. (b) and (d) represent the size distributions of (a) and (c).

dx.doi.org/10.1021/jp202323y |J. Phys. Chem. C 2011, 115, 8988–8993

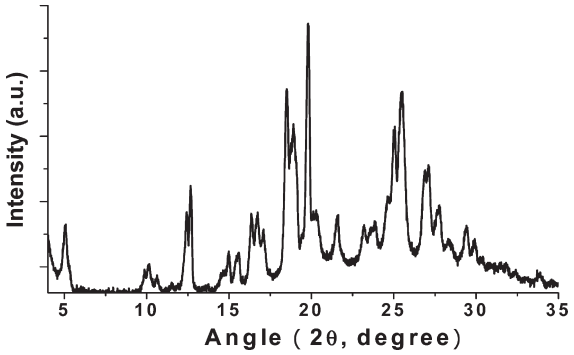

Figure 2. X-ray diffraction (XRD) of DAST ONCs (CSiO-G3/DAST = 8.5:1, [DAST] = 2.0×10^{-5} M). The sample for XRD measurement was prepared by filling the DAST ONCs into a circular sample holder, and the sample surface was roughly flattened using a slide glass. XRD pattern was recorded at a scan rate of 0.1°/s and chopper increment of 0.01°.

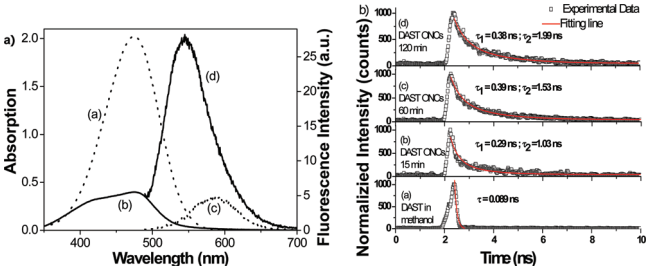

Figure 3. (a) UV−vis absorption spectra (curves a, b) and one-photon excited fluorescence (curves c, d) of DAST methanol solution (2.0×10^{-5} M) (dotted line) and DAST ONCs (2.0×10^{-5} M) (solid line), respectively. The excitation wavelength was 480 nm. (b) Time-resolved fluorescence decay of DAST methanol solution and ONCs with CSiO-G3.

RESULTS AND DISCUSSION

The formation and ripeness of DAST ONCs were found to be improved by the addition of CSiO-G3. The optimum ratio of CSiO-G3/DAST was 8.5. Compared to CSiO-G5 in our previous study,[20] CSiO-G3 was much easier to be synthesized and showed the effective capability in controlling the DAST ONCs growth process. The DAST ONCs were prepared by rapidly injecting 50 μL of DAST methanol solution into 10 mL of diethyl ether (Et_2O) solution of CSiO-G3. The resulting mixture was vigorously stirred with a stirring speed of 1500 rpm for 30 s, and then the mixture was ripened at room temperature.

The configuration of DAST ONCs was well-verified by the characterization of SEM, TEM, and XRD. Figure 1 presents the typical images of ONCs with the CSiO-G3/DAST. The DAST ONCs prepared with CSiO-G3 possessed more regular sphere shape. The size of DAST ONCs was 65 ± 15 nm determined as by SEM (Figure 1a,b). From the TEM image, the DAST ONCs core size achieved was 12 ± 4 nm (Figure 1c,d). The crystal structure was demonstrated by the electron diffraction pattern as shown in Figure 1c (inset). The size difference between SEM and TEM measurements was due to the CSiO-G3 aggregates around DAST ONCs. These results provided the evidence that the CSiO-G3 was effective in the size and shape control of the DAST ONCs, allowing the realization of nanosized ONCs. The XRD showed in Figure 2 indicated that the DAST ONCs belonged to

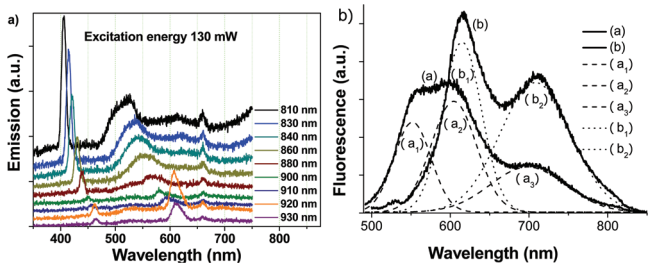

Figure 4. (a) Emission spectra of DAST ONCs dispersion under the two-photon excitation process with different excitation wavelength at 130 mW. (b) Fluorescence emission from solid DAST nanocrystals which was prepared with CSiO-G3/DAST = 8.5:1 (curve a, solid), excited by 475 nm and the emission spectra of bulk crystal (curve b, solid), excited by 474 nm. The solid DAST ONCs exhibited three emission peaks as shown in the fitting curves (a_1, a_2, a_3, dash) and the bulk crystal showed two emission peaks (b_1, b_2, dot).

the monoclinic space group. This result was very close to that of SHG-active bulk crystal and microcrystal,[15] which indicated that the DAST crystal maintained the monoclinic crystal structure even when its size was reduced to nanometric scale.

It was reported that the aggregates of organic molecules would contribute to their emission enhancement.[23] The UV−vis absorption spectra and the one-photon excited fluorescence (OPEF) of DAST ONCs and DAST methanol solution are shown in Figure 3a. The DAST ONCs showed an absorption at 475 nm with a broad width, and the DAST methanol solution was at 474 nm. The shoulder peak appearing at 425 nm was attributed to the H-aggregates of the chromophores.[24] There are two peaks in the absorption spectra of both DAST ONCs and DAST bulk crystals. The same peak presented in both ONCs and DAST bulk crystal at 475 nm is attributed to the absorption of DAST molecule. In addition, the blue-shifted peak at 425 nm due to the H-aggregation was observed in the DAST ONCs while the red-shifted peak at 540 nm in bulk crystals owing to J-aggregation was reported previously.[15] The OPEF spectrum of the DAST ONCs centered at 545 nm with a full width at half-maximum (fwhm) of 108 nm and a quantum yield of 3.5%. In comparison, the DAST methanol solution showed a red-shifted peak at 582 nm with a fwhm of 74 nm and a quantum yield of 0.6%. The fluorescence quantum yield for DAST ONCs was ~6-fold higher than the DAST in methanol solution. Usually, the twisted intramolecular charge transfer (TICT) could induce the fluorescence quenching in solution,[25] especially for neutral molecule. However, DAST, as an ionic molecule, has strong intermolecular interaction by stacking in the nanosized crystals. Therefore, the rotation and vibration, which often induce the fluorescence quenching, can be effectively confined. The confinement of the intermolecular rotation results in the enhancement of the fluorescence quantum yield.

The time-resolved fluorescence decay data were collected at 545 nm for DAST ONCs and 582 nm for DAST methanol solution. As shown in Figure 3b, the fluorescence lifetime of DAST ONCs increased with the increasing of the evolution time. It was obvious that there were two lifetime values during the dispersing process of the DAST ONCs system. After 2 h ripeness, the longer lifetime of DAST ONCs was 1.99 ns and shorter one was 0.38 ns as shown in Figure 3b(d), which were much longer than 0.089 ns for DAST molecule in methanol. It was well-documented that spatial configuration of organic molecules

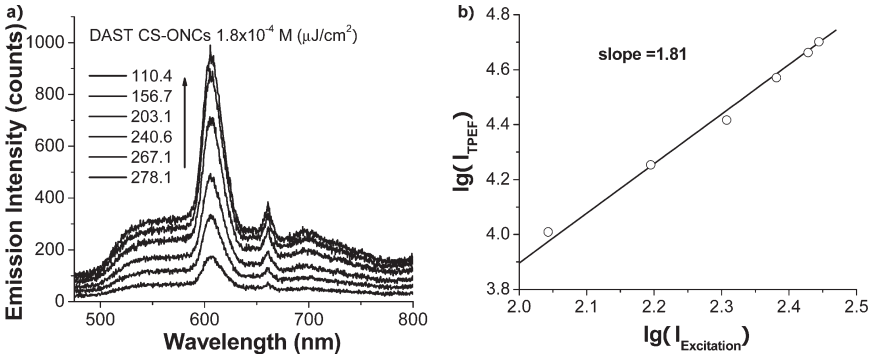

Figure 5. (a) TPEF spectra of DAST ONCs (CSiO-G3/DAST = 8.5:1, 1.8×10^{-4} M) excited at 923 nm with different excitation intensities. (b) TPEF intensity of CSiO-G3/DAST ONCs (CSiO-G3/DAST = 8.5:1, 1.8×10^{-4} M) under different excitation intensities.

played an important role in the stacking mode and the property of the resulting aggregates.[23] DAST molecules aggregated owing to the strong $\pi-\pi$ interaction between DAST molecules in the crystal structure. The unique configuration of DAST ONCs provided a typical organic confinement structure,[12,26] which could be treated as an extended delocalization of π-conjugated system. Therefore, the rotation and vibration of DAST molecules in DAST ONCs could be limited due to the formation of strong $\pi-\pi$ interaction between molecules, which would result in the high fluorescence quantum yield, longer fluorescence lifetime, and better stabilization of the DAST ONCs.

The emission dependence on the excitation wavelength of the DAST ONCs dispersion was demonstrated with multiphoton excitation by using femtosecond laser. Figure 4a shows the emission spectra that irradiated by the different wavelength laser under the same excitation energy. Aside from the strong SHG scattering, surprisingly, the fluorescence emission was red-shifted and changed from broad emission to narrow emission when the excitation wavelength was increased gradually from 810 to 930 nm. The red-shift of the emission peak could result from different energy levels in the relaxation process,[4] which was further verified by the emission spectra from the solid state DAST ONCs as shown in Figure 4b. The fluorescence emission from solid DAST nanocrystals which was prepared with CSiO-G3/DAST = 8.5:1 is shown in spectrum a, excited by 475 nm, and the emission spectra of bulk crystal are shown in spectrum b, excited by 474 nm. The solid DAST ONCs exhibited three emission peaks as shown in the fitting curves (a_1, a_2, a_3), and the bulk crystal showed two emission peaks (b_1, b_2). From the fitting curve, it was obvious that there were three emission peaks in the fluorescence spectra of DAST ONCs at 551, 606, and 703 nm, respectively. In contrast, DAST bulk crystals at solid state only showed two emission peaks at 614 and 706 nm.

A pronounced narrow two-photon emission peak appeared at 606 nm with a fwhm of 17 nm when the DAST ONCs was excited by 923 nm (Figure 5a), even though a broad OPEF peak was observed. As shown in Figure 5a, the TPEF intensity was much stronger compared to the DAST molecules in methanol solution.[20] The dependence of TPEF intensity (I_{TPEF}) on the excitation intensity ($I_{Excitation}$) was analyzed by using logarithm (lg); the plot of lg $I_{Excitation} \sim$ lg I_{TPEF} is obtained in Figure 5b, in which the slope k values of fitting line was 1.81, approaching 2, which demonstrated the quadratic relationship of TPEF on the excitation intensity in the measurement range.

The observation of narrow two-photon excited emission from DAST solution was failed to achieve mainly due to the numerous

Table 1. Optical Properties of DAST ONCs

	Φ_ϕ [b]	τ (ns)[c]	δ (GM)[d]	Φ_ϕ (GM)[e]
solution	0.006	0.089	156	0.936
ONCs	0.035	1.99/0.38	1.72×10^6	6.02×10^4
enhanced factor[a]	5.8	22.4/4.33	6.4	37.3

[a] Enhanced factor of each factor per molecule. [b] Fluorescence quantum yield. [c] Fluorescence lifetime. [d] Two-photon absorption cross section. [e] Two-photon fluorescence action cross section.

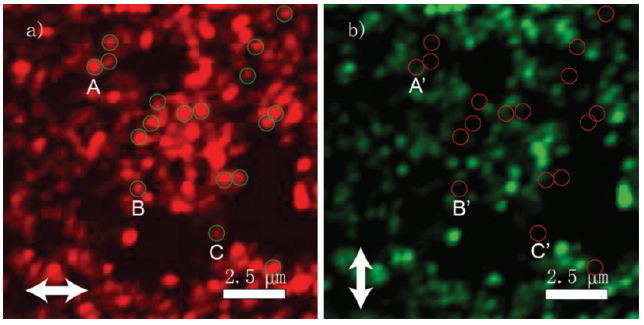

Figure 6. SHG images of DAST ONCs prepared with CSiO-G3. The polarization detections of (a) and (b) were perpendicular to each other. The excitation intensity was 4.5 mW.

energy levels of organic molecules. Accordingly, the π-conjugated structure efficiently restricted the local charge transfer through the $\pi-\pi$ interaction in the $\pi-\pi$ stacking structure of crystal. The dielectric shell made of CSiO-G3 dendrimers interfered with the path of interaction between the π-conjugated nanocrystals and the environment. When the DAST ONCs were excited by the two-photon process, driven by a femtosecond laser pulse with a high light intensity, the configuration significantly reduced the number of split energy states in the relaxation process. Therefore, the molecules were confined distinctly in the lattice with a specific geometric configuration and shared the same energy levels. Moreover, the degree of their variations was drastically reduced, which resulted in the emergence of the narrow two-photon emission.[27]

In order to evaluate the optical enhancement for each molecule, the DAST ONC was considered as a sphere to calculate the number of molecules in a single nanocrystal. From the SEM and TEM results, DAST ONCs had an average size of 65 nm, including a core with an average size of 12 nm and an

dx.doi.org/10.1021/jp202323y |J. Phys. Chem. C 2011, 115, 8988–8993

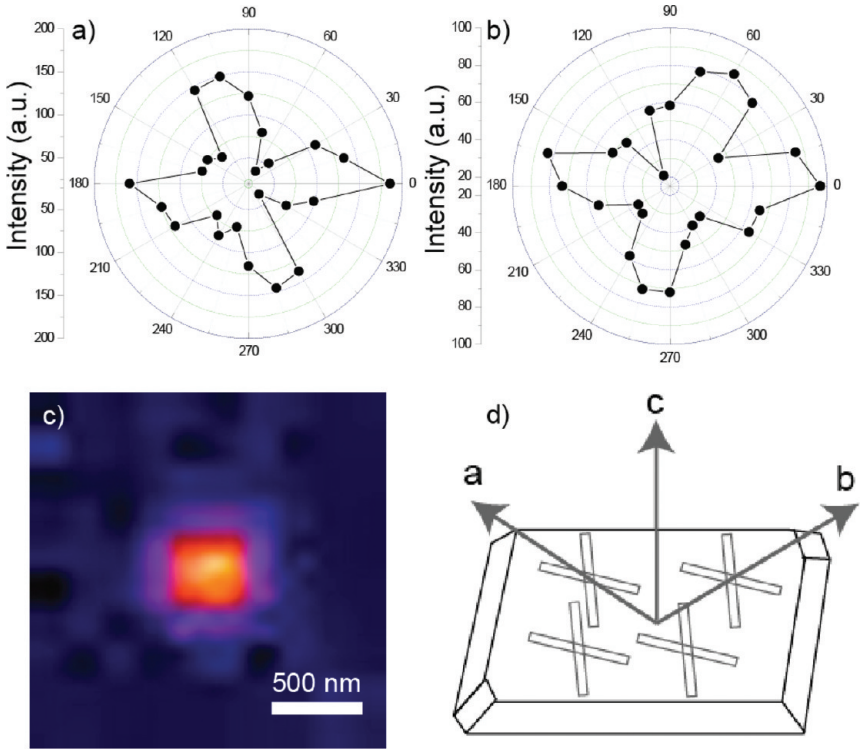

Figure 7. (a, b) Polar graphs of DAST ONCs. The excitation wavelength is 870 nm. (c) Scanning image of SHG emitted from a single DAST ONC, which was bigger than that showed in SEM image due to the diffraction limit of light. (d) Schematic illustration of DAST crystal habit showing the orientation of crystal axes relative to habit geometry.

amorphous CSiO-G3 dendrimer layer with a thickness of about 26.5 nm. According to the parameters of DAST crystal cell,[26,28] a = 10.365 Å, b = 11.322 Å, c = 17.893 Å; the volume of a crystal cell with 4 molecules was about 2.1 nm^3. Consequently, about 1722 DAST molecules were included in one DAST ONC with the average size of 12 nm. Therefore, the concentration of DAST ONCs dispersed in Et_2O was calculated out as 6.99×10^{12} cm^{-3}, corresponding to molar concentration of 2.0×10^{-5} M. The calculated δ of DAST ONCs in diethyl ether was 1.72×10^6 GM, which was more than 10^4 times larger than 156 GM for DAST molecules in methanol. Therefore, the enhancement factor of δ for each molecule in DAST ONCs was 6.4.

The TPEF action cross section, defined as $\delta\Phi_f$, was 6.02×10^4 GM (Table 1) for DAST ONCs, which demonstrated its potential application to fluorescent sensory systems as fluorescence probe in the near-infrared region. The enhancement factor of the absolute TPEF intensity at the same concentration was 37.3, resulting from the cooperative enhancements of both the fluorescence quantum yield and the two-photon absorption cross section.

Besides the investigation of TPEF, the SHG polarization dependence measurement of DAST ONCs to the incident light was further carried out. The SHG images of DAST ONCs that prepared with CSiO-G3 were obtained with the perpendicular polarization detections as shown in Figure 6a,b. The DAST ONCs circled in (a) disappeared in (b), for example, A, B, C in (a) and A′, B′, C′ in (b), when the polarization of the laser changed 90°. Similarly, some DAST ONCs which were circled in (b) disappeared in (a) due to the orientation of DAST ONCs. This result indicated that the DAST ONCs showed polarization dependence to the incident light.

The crystalline feature of a single DAST ONC was further verified by the SHG microscope. The SHG signal was collected by rotating the polarization angle 15° at each incident angle of the excitation laser. The polarization response characteristic of DAST ONCs was representative of its multipolar unit-cell symmetry,[26,28] giving rise to the coupling between polarization directions, which entailed the four-lobe polar graph as illustrated in Figure 7a. This polarization response was corresponding to that of the bulk crystal.[29] Note that the size of the single crystal shown in Figure 7c was bigger than that obtained in SEM image due to the diffraction limit of light. For the same single DAST ONC, the SHG intensity was different when the signal was collected from different directions. For example, in Figure 7b, the SHG signal changed when the direction of the detection rotated 90° from (a). The result here indicated that the pattern of the polar graph was very sensitive to the polarization direction of detection and the orientation of the crystal axes (Figure 7d).

CONCLUSIONS

In conclusion, we have investigated the nonlinear optical properties of DAST ONCs, which were successfully prepared with dendrimer CSiO-G3. The crystal structure of DAST ONCs has been demonstrated by XRD and TEM as a monoclinic space group. The DAST ONCs showed 6-fold larger fluorescence quantum yield and prolonged fluorescence lifetime compared to DAST molecular solution. The TPEF intensity of the DAST ONCs was improved by a factor of 37.3 compared to the DAST molecules in methanol solution. The extraordinary large two-photon absorption cross section up to 1.72×10^6 GM was obtained. The four-lobe polarization pattern in the SHG

microscopy investigation represented the multipolar unit cell of single DAST ONC. The fluorescence enhancement and the polarization dependence of the DAST ONCs would provide the opportunity for their potential application in fluorescent sensing or switching, up-converted lasing, and nonlinear optics.

■ ASSOCIATED CONTENT

Supporting Information. Details of the molecular structure (Scheme S1) and dynamics of the growth process (Figure S1). This material is available free of charge via the Internet at http://pubs.acs.org.

■ AUTHOR INFORMATION

Corresponding Author

*E-mail: fujita@ap.eng.osaka-u.ac.jp (K.F.), xmduan@mail.ipc.ac.cn (X.-M.D.).

■ ACKNOWLEDGMENT

We thank Professor Masanori Ozaki at Osaka University for help with time-resolved fluorescence measurements. This work was financially supported by project (06B44523a) of Japan, the Knowledge Innovation Program of CAS (KJCX.2.YW.M04), NSFC (20702056, 50773091, 50973126), 973 (2010CB934103), and ICP (2008DFA02050) programs of MOST.

■ REFERENCES

(1) Mongin, O.; Krishna, T. R.; Werts, M. H. V.; Caminade, A.-M.; Majoral, J.-P.; Blanchard-Desce, M. *Chem. Commun.* **2006**, 915.

(2) Krishna, T. R.; Parent, M.; Werts, M. H. V.; Moreaux, L.; Gmouth, S.; Charpak, S.; Caminade, A.-M.; Majoral, J.-P.; Blanchard-Desce, M. *Angew. Chem., Int. Ed.* **2006**, *45*, 4645.

(3) Ventelon, L.; Charier, S.; Moreaux, L.; Mertz, J.; Blanchard-Desce, M. *Angew. Chem., Int. Ed.* **2001**, *40*, 2098.

(4) Zhao, L.-J.; Xu, J.-J.; Zhang, G.-Y.; Bu, X.-H.; Shionoya, M. *Opt. Lett.* **1999**, *24*, 1793.

(5) Fang, H.-H.; Chen, Q.-D.; Yang, J.; Xia, H.; Ma, Y.-G.; Wang, H.-Y.; Sun, H.-B. *Opt. Lett.* **2010**, *35*, 441.

(6) Horn, D.; Rieger, J. *Angew. Chem., Int. Ed.* **2001**, *40*, 4330.

(7) Kim, S.; Zheng, Q.; He, G. S.; Bharali, D. J.; Pudavar, H. E.; Baev, A.; Prasad, P. N. *Adv. Funct. Mater.* **2006**, *16*, 2317.

(8) Lim, S.-J.; An, B.-K.; Jung, S. D.; Chung, M.-A.; Park, S. Y. *Angew. Chem., Int. Ed.* **2004**, *43*, 6346.

(9) An, B.-K.; Kwon, S.-K.; Park, S. Y. *Angew. Chem., Int. Ed.* **2007**, *46*, 1978.

(10) Lacerda, S. H. D. P.; Douglas, J. F.; Hudson, S. D.; Roy, M.; Johnson, J. M.; Becker, M. L.; Karim, A. *ACS Nano* **2007**, *1*, 337.

(11) Reeve, J. E.; Collins, H. A.; Mey, K. D.; Kohl, M. M.; Thorley, K. J.; Paulsen, O.; Clays, K.; Anderson, H. L. *J. Am. Chem. Soc.* **2009**, *131*, 2758.

(12) Marder, S. R.; Perry, J. W.; Schaeffer, W. P. *Science* **1989**, *245* 626.

(13) Fujita, S.; Kasai, H.; Okada, S.; Oikawa, H.; Fukuda, T.; Matsuda, H.; Tripathy, S. K.; Nakanishi, H. *Jpn. J. Appl. Phys.* **1999**, *38* 659.

(14) Kaneko, Y.; Shimada, S.; Fukuda, T.; Kimura, T.; Yokoi, H.; Matsuda, H.; Onodera, T.; Kasai, H.; Okada, S.; Oikawa, H.; Nakanishi, H. *Adv. Mater.* **2005**, *17*, 160.

(15) Oikawa, H.; Fujita, S.; Kasai, H.; Okada, S.; Tripathy, S. K.; Nakanishi, H. *Colloids Surf., A* **2000**, *169*, 251.

(16) Duan, X.-M.; Konami, H.; Okada, S.; Oikawa, H.; Matsuda, H.; Nakanishi, H. *J. Phys. Chem.* **1996**, *100*, 17780.

(17) Adachi, H.; Takahashi, Y.; Yabuzaki, J.; Mori, Y.; Sasaki, T. *J. Cryst. Growth* **1999**, *198*, 568.

(18) Zheng, M.-L.; Chen, W.-Q.; Duan, X.-M. *J. Phys. Chem. A* **2008**, *112*, 6864.

(19) Zheng, M.-L.; Chen, W.-Q.; Li, C.-F.; Dong, X.-Z.; Duan, X.-M. *ChemPhysChem* **2007**, *8*, 810.

(20) Zheng, M.-L.; Chen, W.-Q.; Fujita, K.; Duan, X.-M.; Kawata, S. *Nanoscale* **2010**, *2*, 913.

(21) Smith, D. K. *Chem. Commun.* **2006**, 34.

(22) Frey, H.; Schlenk, C. *Top. Curr. Chem.* **2000**, *210*, 69.

(23) Kim, S.; Pudavar, H. E.; Bonoiu, A.; Prasad, P. N. *Adv. Mater.* **2007**, *19*, 3791.

(24) Mann, J. R.; Gannon, M. K.; Fitzgibbons, T. C.; Detty, M. R.; Watson, D. F. *J. Phys. Chem. C* **2008**, *112*, 13057.

(25) Grabowski, Z. R.; Rotkiewicz, K.; Rettig, W. *Chem. Rev.* **2003**, *103*, 3899.

(26) Marder, S. R.; Perry, J. W.; Yakymyshyn, C. P. *Chem. Mater.* **1994**, *6*, 1137.

(27) Zhao, Y. S.; Xiao, D.; Yang, W.; Peng, A.; Yao, J. *Chem. Mater.* **2006**, *18*, 2302.

(28) Pan, F.; Wong, M. S.; Bosshard, C.; Günter, P. *Adv. Mater.* **1996** *8*, 592.

(29) Komorowska, K.; Brasselet, S.; Dutier, G.; Ledoux, I.; Zyss, J.; Poulsen, L.; Jazdzyk, M.; Egelhaaf, H.-J.; Gierschner, J.; Hanack, M. *Chem. Phys.* **2005**, *318*, 12.